

Fermi surface of Co(0001) and initial-state linewidths determined by soft x-ray angle-resolved photoemission spectroscopy

M. Mulazzi,¹ J. Miyawaki,¹ A. Chainani,^{1,2} Y. Takata,^{1,2} M. Taguchi,¹ M. Oura,^{1,2} Y. Senba,³ H. Ohashi,³ and S. Shin^{1,4}

¹*Excitation Order Research Team, RIKEN SPring-8 Centre, Sayo-cho, Hyogo 679-5148, Japan*

²*Coherent X-ray Optics Group, RIKEN SPring-8 Centre, Sayo-cho, Hyogo 679-5148, Japan*

³*JASRI/SPring8, Sayo-cho, Hyogo 679-5198, Japan*

⁴*The University of Tokyo, Institute of Solid State Physics, Kashiwanoha, Kashiwa, Chiba, 277-8581, Japan*

(Received 13 September 2009; published 15 December 2009)

Soft x-ray angle-resolved photoemission spectroscopy (SX-ARPES) reveals the band dispersion and Fermi surface of bulk ferromagnetic Co(0001). The spectral peak widths are narrower than previously observed in low-energy ARPES experiments. From very general considerations and in contrast to low-energy experiments, we show that the final-state broadening is significantly reduced in the experimentally measured linewidth. SX-ARPES yields the intrinsic initial-state lifetime $\Gamma_i = 1/2\Sigma_i(\vec{k}, E)$, the latter being the initial state self-energy, quantifying the correlations and indicating an energy and momentum dependence. Our results open a way to a direct measurement of the many-particle effects in solid-state physics, which does not require a modeling of the final state and provides a genuine description of the initial state.

DOI: [10.1103/PhysRevB.80.241106](https://doi.org/10.1103/PhysRevB.80.241106)

PACS number(s): 71.20.Be, 71.18.+y, 79.60.-i

I. INTRODUCTION

One of the most active fields in contemporary physics is the study of strong correlations in solids, greatly contributing to the behavior of important materials like high-temperature superconductors. Many fundamental ideas in this field have been obtained using angle-resolved photoemission spectroscopy (ARPES) which measures the photoelectron intensity distribution as a function of the emission angle and kinetic energy. Since the excited photohole and photoelectron are able to exchange energy and momentum with each other and with the remaining electrons,¹⁻³ photoemission actually measures a complex initial-to-final-state transition. In the approximation in which the hole is sufficiently screened, the ground (or initial) state band structure can be measured and the emission angle and kinetic energy can be related to electron states with specific energy and momentum. Moreover, by the analysis of the photoemission peak linewidth it is possible to infer the electron self-energy $\Sigma(\vec{k}, E)$ representing the many-body interactions (electron-electron, electron-phonon, electron-plasmon, etc.) that are relevant to the description of the electronic structure.⁴⁻⁶ The system under study, cobalt, is an itinerant strong ferromagnet (with the majority spin band almost completely filled) having an hexagonal close-packed unit cell with a magnetocrystalline anisotropy inducing an easy magnetization axis parallel to the (0001) direction.⁷ As for other itinerant ferromagnetic 3d metals, the electronic structure description requires the introduction of correlations among the valence-band electrons. The exchange interaction splits the otherwise degenerate spin-up and spin-down bands by an energy separation, called exchange splitting, that is related to the Curie temperature and the saturation magnetization. Cobalt, has the highest ferromagnetic Curie temperature ($T_C=1388$ K) among the elemental metals, even higher than that of Iron ($T_C=1043$ K), in spite of a lower magnetic moment. Surprisingly, it has not been possible to map the Fermi surfaces of bulk hcp cobalt using ARPES, yet. High-resolution low-energy ARPES study⁸ showed the absence of quasiparticle

bands at binding energies $E_B > 2$ eV. It was suggested that strong spin-dependent many-body interactions lead to a quenching of the majority channel excitations in Co. A more recent study with low-energy ARPES on tetragonally distorted fcc cobalt film on copper⁹ showed that final-state effects dominate the spectra, thus limiting the ability of Fermi-surface mapping. In this work we revisit the electronic structure of Co(0001) single crystal using soft x-ray (SX)-ARPES: because of the advantages offered by the use of high energy photons and using advanced photoelectron analyzers it is now possible to measure the electronic structure along one high-symmetry direction of the Brillouin zone in a single measurement, though paying a price in terms of momentum broadening and energy resolution.¹⁰⁻¹⁵ Thanks to the rather high photon energy ($488 < h\nu < 654$ eV) and special experimental geometry, new details of the Fermi surface and band dispersion were measured. These results do not originate from higher energy or momentum resolutions or better surface quality, but by the reduction of the photoemission peak widths in the soft x-ray than in the UV regime.^{16,17} The reason for the narrower linewidths is attributed to the significant suppression of the final-state broadening when measured with soft x-rays and the consequent reduction of the total linewidth, which is due to the initial state only. For this reason, SX-ARPES opens a way to determine the correlation effects directly from the experiments in terms of the real and imaginary parts of the self-energy.

II. EXPERIMENTAL

The Co(0001) crystal was prepared by several sputtering (with Argon ions at 0.6 keV) and annealing (at 330 °C, limited by the structural phase transition¹⁸) cycles before collecting the ARPES data. Low-energy electron diffraction images revealed only the hcp spots, indicating a well-defined lattice structure. All the data presented here were collected within 8 h after the surface preparation and during that period no Oxygen or Carbon signal could be detected. The SX-ARPES measurements were carried out at the b-branch

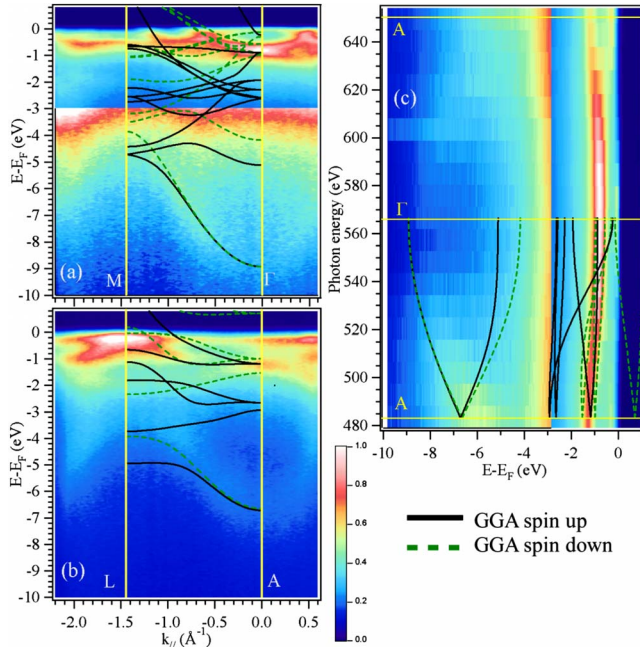


FIG. 1. (Color online) SX-ARPES maps measured as a function of the binding energy and k_{\parallel} for two different values of k_{\perp} : (a) along the ΓM (with $h\nu=570$ eV), (b) AL (with $h\nu=654$ eV). (c) shows an ARPES map along the $A\Gamma A$ direction (k_{\perp}) obtained by changing the photon energy. The color scale is shown between the panel (b) and (c). In (b) and (c) the intensities at $E_B > 3$ eV are plotted in a different color scale to enhance the weak sp band. In all the three panels GGA calculations (spin-up bands in black continuous and spin-down bands in dashed green lines) are overlapped for comparison.

of the BL17SU beamline at SPring-8 which provides soft x-rays in the 300–2000 eV energy range.¹⁹ By keeping the photon beam at $\approx 5^\circ$ from the sample surface, the asymmetry factor of the photoelectron distribution maximizes the photoelectron intensity for a given photon flux,²⁰ thus allowing 120 meV and 0.2° resolutions, and ≈ 30 min acquisition time for each ARPES map. The photoelectrons of wave vectors belonging to the ΓM and AL directions could be collected at the same time in the $\pm 6^\circ$ range of the Scienta 2002 analyzer. We used circularly polarized photons in order to avoid the on/off effect of selection rules on electron bands of given symmetry arising in photoemission with linear polarization. Given the relatively high Debye temperature of cobalt, $\Theta_D=385$ K, the weight of direction transition can be estimated^{10,13,14} to be the 85% of the total intensity, for $h\nu=500$ eV, $T=50$ K.

III. RESULTS

We present the SX-ARPES data obtained as functions of k_{\parallel} in Figs. 1(a) Fig. 1(b) along two high-symmetry directions, ΓM and AL , and k_{\perp} along $A\Gamma A$ in Fig. 1(c). In early works using low-energy ARPES,^{8,16,17,21} the photoemission intensity was almost completely blurred at binding energies higher than 2 eV, but in the SX-ARPES data it is possible to observe (relatively broad) peaks up to $E_B=9$ eV.

In Figs. 1(a) and 1(b) it is possible to see the band dispersion of the d states within ~ 4 eV from the Fermi level and the sp bands from 4 to 9 eV binding energy. The latter has a very k -dependent intensity, becoming weaker at the Γ point and stronger near the M point [as seen in Fig. 1(a)] and at the A point [as seen in Fig. 1(c)]. We attribute such a behavior to matrix element effects, as was found for the case of Al(100) (Ref. 22) in the same photon energy range.

Apart from k -dependent matrix elements, the sp band can be measured because the Coulomb interaction mainly affects the localized d states, while affecting less the almost-free-electron sp bands. For this reason the sp band peaks could be detected, even if their intensity is much weaker and their width is larger than the d bands.

The blurring of the photoemission peaks in cobalt (and also Nickel) at high binding energies was interpreted by the 3BS theory in terms of different final-state scattering rates for majority and minority spins^{8,23} caused by the presence of two holes in the minority band. In a different theoretical framework, a spin-dependent self-energy was calculated by dynamical mean-field theory (DMFT) (Ref. 24) and found to be larger for majority-spin electrons. While this argument finds a confirmation in our data, we notice in Figs. 1(a), 1(c), and 3 that the strongest feature of SX-ARPES spectrum at Γ is nearly 0.5eV wide, while widths of 0.7,¹⁶ 0.8,⁸ and 0.78eV (Ref. 17) are reported in the literature. We stress that in our experiments the energy resolution is $\Delta E \approx 120$ meV, comparable to the one of Ref. 16, while other experimental works featured $\Delta E=50$ meV (Ref. 8) and $\Delta E=40$ meV.¹⁷ Similarly, at the M point we get resolution-limited peaks of ≈ 120 meV (at binding energies of about 0.2 and 0.6 eV), as shown in Fig. 3.

The calculations shown in Fig. 1 are the results of density-functional theory in the generalized gradient approximation (GGA) scheme applied to bulk Co(0001) with the magnetization parallel to the (0001) axis and using the experimental lattice parameters.²⁵ The GGA band dispersions are compatible with earlier⁸ work and were used to identify the spin and orbital character of the experimental bands.²⁹ Moreover, in the SX-ARPES measurements, well-defined quasiparticle peaks are observed in a wider energy range and also at (in the ΓMK plane) momenta larger than 1.8 \AA^{-1} . In contrast, low-energy data do not show well-defined peaks at momenta larger than 1.3 \AA^{-1} , even for bands near the Fermi level, where the linewidth should become virtually zero. The spectrum at the Γ point shows an intense peak at about $E_B=1$ eV and a sharp feature just below the Fermi level that was observed as a shoulder in the previous experiments. Because of the well-defined peaks we could investigate the Fermi surface of cobalt in both the ΓMK and ΓALM planes, as shown in Fig. 2, finding very different results with respect to the above-quoted experimental works. The measured Fermi surface is compatible with our calculations.²⁹

The reason for the broad Fermi-surface features reported in the literature¹⁷ was attributed to the magnetic stray field coming from the sample magnetization oriented perpendicular to the surface. In our case, the higher kinetic energies and the magnetization direction lying within $\approx 6^\circ$ from the photoelectron momentum should reduce the effect of the stray magnetic field by more than 90%. The Lorentz force should

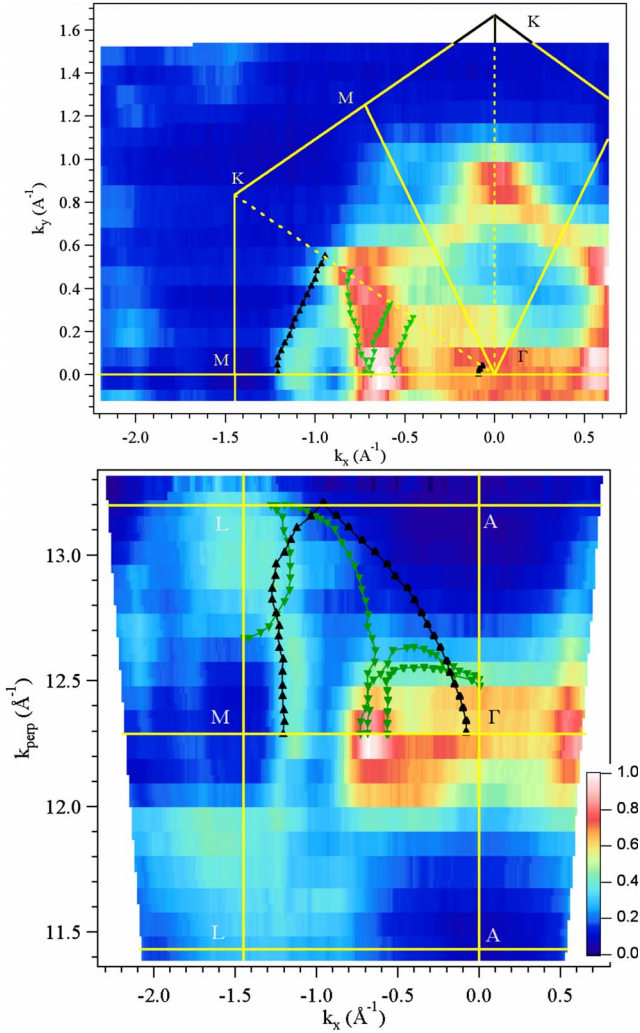


FIG. 2. (Color online) Cobalt Fermi-surface mappings measured in the ΓMK plane with $h\nu=570$ eV (top) and in the ΓALM plane as a function of the photon energy (bottom) by stacking MDCs obtained by integrating over ± 50 meV about the Fermi level. The Brillouin-zone high-symmetry directions are indicated by yellow lines, while the spin-up (up black triangles) and spin-down (down green triangles) mark the theoretical Fermi-surface contours derived from our GGA calculations (indicated in only one irreducible wedge of the Brillouin zone, to avoid redundancy). The color scale is indicated at the bottom right.

give a negligible contribution to the SX-ARPES from Co(0001) single crystals collected in the described geometry.

Fermi-surface measurement in the low-energy regime was carried out also by Gao *et al.*⁹ who concluded that the photoemission final states mainly determine the experimental shape of the Fermi surface, with almost no resemblance to the initial states. The striking difference between the data of Fig. 2 and the low-energy results is caused by final-state effects that are strongly reduced for soft x-rays experiments, but relevant in the low-energy regime. This conclusion is based on the following formula:²⁶ $\Gamma_{exp} = \Gamma_i + \left| \frac{v_{i,\perp}}{v_{f,\perp}} \right| \Gamma_f$ in which Γ_i and Γ_f are the initial and final-state (hole and photoelectron) broadening and $v_{i(f),\perp}$ are the initial (final) state group-velocity components perpendicular to the surface. The above formula is a special case valid at normal emission of a more

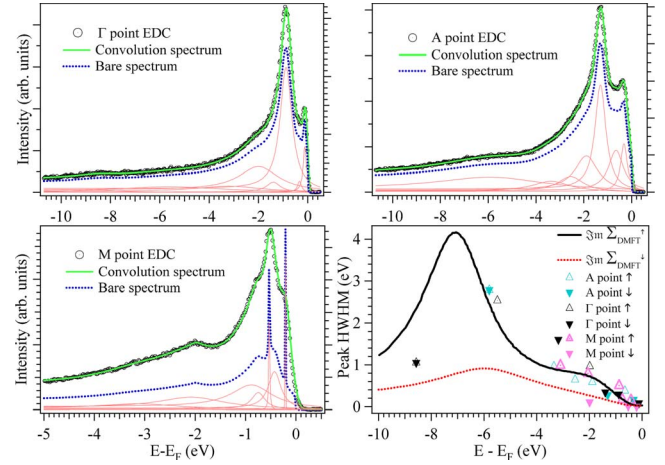


FIG. 3. (Color online) Experimental EDCs (black open circles) taken at the Γ , A, and M points plotted together with the convolved (light green or gray thick continuous line) and bare spectrum (blue or dark gray dashed line), composed of a sum of Lorentzian peaks (thin red or light gray lines). In the bottom right panel the DMFT calculations (Ref. 24) (black continuous line for spin-up and red or gray dashed line for spin-down) and the experimental widths for both spin-up (up triangles) and spin-down (down triangles) are compared. The error bar on the peak widths is as large as the symbols and is given by the experimental energy resolution, not by the (smaller) error on the parameter determined by the fit.

general model²⁸ of the photoemission process. Up to now, it was considered useful only for two-dimensional systems in which $v_{i,\perp} = 0$. However, in the soft x-rays regime, the final state can be approximated by a plane wave and because of the high energy, the ratio $\frac{v_{i,\perp}}{v_{f,\perp}} \propto \frac{1}{k_{\perp}} \approx \frac{1}{13} \approx 0.08$ for photoelectrons of 650 eV kinetic energy. In Ref. 27 the kinematical compression of photoemission peaks derived from bands at very specific k-points such that $v_{i,\perp} \approx 0$ and large $v_{i,\parallel}$ at grazing emission was understood as a special case of the general model of Ref. 28. In our case since the emission is never grazing (but limited to a small-angle near normal emission) and narrow peaks are observed at all the k-points of the Brillouin zone we conclude that the kinematical compression is not the origin of the peak narrowing.

Thus in the soft x-ray regime, the measured lifetime is dominated by the initial state one when the measurements are done at normal emission (off normal emission the lifetime is broadened by a negligible geometrical factor, given the small angles needed to map the Brillouin zone).²⁹ On the other hand, in the VUV regime the final-state lifetime gives the largest contribution to the total linewidth. Consequently, the SX-ARPES measures the initial-state correlations with no need to model the final state, thus promoting SX-ARPES to a very powerful tool for the investigation of many-particle phenomena. By these considerations on the lifetime and the similarity between band-structure calculations with our Fermi-surface mapping, we confirm that earlier published photoemission data of cobalt are mainly dominated by final-state effects when measured in the low-energy regime.

Since the photoelectron broadening is naturally removed in SX-ARPES and the instrumental energy resolution is well known, we fitted the energy distribution curves (EDCs) taken

at the Γ , A and M points to obtain the peak widths of the “ideal” spectrum (the one that would be measured with an infinitely resolving instrumentation). The procedure to obtain the initial-state linewidths consisted in fitting the experimental EDCs to a bare spectrum (a sum of Lorentzian functions multiplied by the Fermi-Dirac distribution calculated at the experimental temperature) convolved with a Gaussian function simulating the total-energy resolution of the experimental apparatus ($\Delta E \approx 120$ meV resolution Gaussian but at the M point where $\Delta E \approx 160$ meV). The details of the fit procedure, stability and error treatment is discussed in the Ref. 29. The observed linewidths are in very good agreement with the DMFT calculations²⁴ for both the majority and minority-spin bands, as seen in the lower right part of Fig. 3. In particular the minority-spin band at 2 eV measured at the M point is correctly predicted by the DMFT to have a small width (about 150 meV). The lack of experimental peaks at energies between 3 and 6 eV forbids verifying if the linewidth increases linearly or with the more complex behavior predicted by the DMFT. The agreement up to 3 eV binding energy between the experiment and the theory is even more formidable considering that the calculated self-energy $\Sigma_i(E)$ is only spin and energy dependent but not momentum dependent.

From the experimental data it is possible to quantify the exchange splitting of the cobalt d bands in $\Delta^{exp} = 1.05$ eV, estimated from the identification of the spin-up and spin-down bands. The DMFT calculations give for the d bands $\Delta^{th} = 1.3$ eV, in good agreement with the experimental one.

The exchange splitting is very small for sp compared to d bands, as in the case of Nickel.³⁰

We summarize saying that we measured the band dispersion and Fermi surface of a Co(0001) single crystal with soft X-rays in the 488–654 eV energy region using an experimental geometry drastically reducing the potential artifacts induced by the magnetization and ensuring a photoelectron intensity comparable to that of low-energy photoemission beamlines. The experimental Fermi surface is in qualitative agreement with density-functional theory calculations, but different from the ARPES data obtained using low-energy photons. The differences among the experiments were explained by a simple model evidencing that the SX-ARPES measured linewidth can be directly compared to initial-state linewidth calculations. The experimental linewidths obtained by a fitting procedure were found to be in very good agreement with state-of-the-art DMFT calculations up to binding energies of 3 eV. With energy resolutions reduced to ≈ 20 meV, SX-ARPES could measure very precise initial-state lifetimes for direct comparison with self-energy calculations.

ACKNOWLEDGMENT

This work was supported by the Foreign Postdoctoral Researchers Program of RIKEN. The synchrotron radiation experiments (Proposal No. 20080050) were performed with the approval of RIKEN.

- ¹K. M. Shen *et al.*, Phys. Rev. Lett. **93**, 267002 (2004).
- ²T. Valla *et al.*, Science **285**, 2110 (1999).
- ³K. Ishizaka *et al.*, Phys. Rev. Lett. **100**, 166402 (2008).
- ⁴A. Bostwick *et al.*, Nature Phys. **3**, 36 (2007).
- ⁵A. Lanzara *et al.*, Nature (London) **412**, 510 (2001).
- ⁶J. Schäfer, D. Schrupp, E. Rotenberg, K. Rossnagel, H. Koh, P. Blaha, and R. Claessen, Phys. Rev. Lett. **92**, 097205 (2004).
- ⁷N. W. Ashcroft and N. D. Mermin, *Solid State Physics* (Holt-Saunders, Philadelphia, 1976).
- ⁸S. Monastera, F. Manghi, C. A. Rozzi, C. Arcangeli, E. Wetli, H. J. Neff, T. Greber, and J. Osterwalder, Phys. Rev. Lett. **88**, 236402 (2002).
- ⁹X. Gao, A. N. Koveshnikov, R. H. Madjoe, R. L. Stockbauer, and R. L. Kurtz, Phys. Rev. Lett. **90**, 037603 (2003).
- ¹⁰F. Venturini, J. Minar, J. Braun, H. Ebert, and N. B. Brookes, Phys. Rev. B **77**, 045126 (2008).
- ¹¹L. E. Klebanoff and D. G. Van Campen, Phys. Rev. B **46**, 9744 (1992).
- ¹²S. Suga *et al.*, Phys. Rev. B **70**, 155106 (2004).
- ¹³L. Plucinski, J. Minar, B. C. Sell, J. Braun, H. Ebert, C. M. Schneider, and C. S. Fadley, Phys. Rev. B **78**, 035108 (2008).
- ¹⁴M. Månsson, T. Claesson, M. Finazzi, C. Dallera, N. B. Brookes, and O. Tjernberg, Phys. Rev. Lett. **101**, 226404 (2008).
- ¹⁵R. Eguchi, A. Chainani, M. Taguchi, M. Matsunami, Y. Ishida, K. Horiba, Y. Senba, H. Ohashi, and S. Shin, Phys. Rev. B **79**, 115122 (2009).
- ¹⁶F. J. Himpsel and D. E. Eastman, Phys. Rev. B **21**, 3207 (1980).
- ¹⁷E. Wetli, T. J. Kreuz, H. Schmid, T. Greber, J. Osterwalder, M. Hochstrasser, Surf. Sci. **402-404**, 551 (1998).
- ¹⁸M. Erbudak, E. Wetli, M. Hochstrasser, D. Pescia, and D. D. Vvedensky, Phys. Rev. Lett. **79**, 1893 (1997).
- ¹⁹H. Ohashi *et al.*, *AIP Conf. Proc.* No. 879 (AIP, New York, 2007), p. 523.
- ²⁰N. Kamakura, Y. Takata, T. Tokushima, Y. Harada, A. Chainani, K. Kobayashi, and S. Shin, Phys. Rev. B **74**, 045127 (2006).
- ²¹F. J. Himpsel and D. E. Eastman, Phys. Rev. B **20**, 3217 (1979).
- ²²P. Hofmann, C. Sondergaard, S. Agergaard, S. V. Hoffmann, J. E. Gayone, G. Zampieri, S. Lizzit, and A. Baraldi, Phys. Rev. B **66**, 245422 (2002).
- ²³J. Osterwalder, J. Electron Spectrosc. Relat. Phenom. **117-118**, 71 (2001).
- ²⁴A. Grechnev, I. Di Marco, M. I. Katsnelson, A. I. Lichtenstein, J. Wills, and O. Eriksson, Phys. Rev. B **76**, 035107 (2007).
- ²⁵P. Blaha *et al.*, in *WIEN2k, An Augmented Plane Wave and Local Orbitals Program for Calculating Crystal Properties*, edited by K. Schwarz (Technische Universität, Vienna, 2001).
- ²⁶F. Reinert and S. Hüfner, in *Very High Resolution Photoelectron Spectroscopy*, Lecture Notes in Physics Vol. 715, (Springer, Berlin, 2007), p. 13.
- ²⁷E. D. Hansen, T. Miller, and T. C. Chiang, Phys. Rev. Lett. **80**, 1766 (1998).
- ²⁸N. V. Smith *et al.*, Phys. Rev. B **47**, 15476 (1993).
- ²⁹See EPAPS Document No. E-PRBMDO-80-R33944 for the supplementary materials included in this Rapid Communication. For more information on EPAPS, see <http://www.aip.org/pubservs/epaps.html>
- ³⁰T. J. Kreuz *et al.*, Phys. Rev. B **58**, 1300 (1998).